DINAME 2019 - Proceedings of the XV International Symposium on Dynamic Problems of Mechanics,
M.A. Savi, T.G. Ritto and W.M. Bessa (Editors), ABCM, Buzios, RJ, Brazil, March 10th to 15th, 2019

Dynamic strain analysis using spectral element method

Thiago Pereira e Silva [1], Marcela Rodrigues Machado[1], Leila Khalij[2]

[1] Universidade de Brasília, Campus Universitário Darcy Ribeiro, CEP 70910-900, Brasília-DF, Brasil.

[2] Normandie Université, LMN/INSA Rouen Normandie, 76000 Rouen, France.

The spectral element method (SEM) is a computational tool that has been successfully used in the model and evaluate the response of the wave propagation in structures. Considering that strain is an important feature of the material to a load, be it static or cyclic and can be used in studies of static failure or fatigue phenomenon, this work used the SEM to evaluate the dynamic strain. The SEM is used to model a healthy homogeneous and isotropic beam. The strain frequency response function (SFRF) is applied in the study as a manner of identifying the mechanical behavior of structure such as its dynamics properties, mode shape, natural frequencies. The efficiency of this proposed method is validated by comparison with an experimental simulation. The comparison of the results shows that the SEM is an efficient method considering the proximity of results, and the direct measurement of the dynamic strain.

Keywords: Spectral Element Method, Dynamic Strain, Wave propagation.

INTRODUCTION

In the industry and mechanical researching, is highly important the existence of non-destructive methods that decrease the investigation cost when treated of the structure. The healthily of a structure is directly linked to maintenance and dynamic analysis. As a tool to realize this analysis, the spectral element method (SEM) is an efficient method.

The spectral element method (SEM) is an alternative method to analyze wave propagation in place of finite element method (FEM) that works with many nodes to analyze simple and complex geometries (Doyle, 1997). The formulation of SEM begins with an exact solution to governing partial differential equations (PDE) in the frequency domain. To interpolation function for spectral element formulation, the exact solution is used (Machado, 2012). Using an exact solution ensures exact mass and stiffness distribution, bringing a result as element directly yields the exact dynamic stiffness matrix. Hence, the problem dimensions are very trivial compared to conventional FE formulation even for compelling functions having large frequency content (Lee, 2009).

Strain measurement has been commonly used for static load testing in the industry and academic environment. Moreover, fatigue testing, durability analysis, and lifetime prediction have also been a common application where strain gauges are used. This sort of testing is a common part of the product development process, and additional information on product durability and dynamic performance can be assessed by obtaining the modal parameters of the system, while still using the same instrumentation (Santos, 2011).

In this work, the SEM is going to use to model the dynamic behavior of a Euler-Bernoulli beam, with a homogeneous and isotropic material. The results are validated by comparison with a recent work where the author did the new approach for the normalization of strain modes for beams, and the validation of reciprocity as long as some location conditions on the beam. The validation of SFRFs is realized comparing experimental results, obtained by literature (Santos, 2011), and numerical results using SEM.

SPECTRAL ELEMENT METHOD

The spectral element method is like the finite element method (FEM), the main difference is in the stiffness matrix, that is established in the frequency domain (Doyle, 2009). The inertia of the distributed mass is described exactly due to this. Therefore, these spectrally formulated elements exactly describe the wave propagation dynamics, and this means that elements can be distributed in decreases number of nodes without losing fidelity. There are many kinds to establish a dynamic stiffness, but in this paper, we going to use the dynamic shape functions. They are the interpolation function between the elements ends, but in this way, the exact displacement distributions are used instead of simple polynomials.

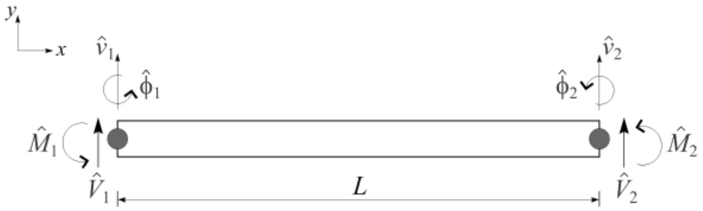

Figure 1 – Spectral element of Euler-Bernoulli beam.

Considering a homogeneous and isotropic beam, that have constant properties along the length, then the homogeneous differential equation is written in the spectral form as (Doyle, 2009),

$$\frac{d^4\hat{v}}{dx^4} - \beta^4\hat{v} = 0 \tag{1}$$

where,

$$\beta^2 = \sqrt{\frac{\omega^2\rho A - i\omega A}{EI}} \tag{2}$$

where ω is the angular frequency, ρ mass density, A cross section area, E Young Modulus, I second moment of area. Relating the two equations following, to its particular solutions we can obtain particular solutions to Eq.(1),

$$\frac{d^2\hat{v}}{dx^2} + \beta^2\hat{v} = 0 \tag{3}$$

and,

$$\frac{d^2\hat{v}}{dx^2} - \beta^2\hat{v} = 0 \tag{4}$$

using the solution as e^{-ikx}, substituting into the equations gives

$$k_1 = \pm\beta, \qquad k_2 = \pm i\beta$$

the complete solution is,

$$v(x,t) = \sum[Ae^{-i\beta x} + Be^{-\beta x} + Ce^{+i\beta x} + De^{+\beta x}]e^{i\omega t} \tag{5}$$

Shape function

In the Bernoulli-Euler beam, just the flexural stress is considered, so the transverse displacement of the beam can be written in the form,

$$\hat{v}(x) = \hat{g}_1(x)\hat{v}_1 + \hat{g}_2(x)L\hat{\phi}_1 + \hat{g}_3(x)\hat{v}_2 + \hat{g}_4(x)L\hat{\phi}_2 \tag{6}$$

for the two-nodded element, the frequency dependent shape functions are given as

$$\hat{g}_1(x) = r_1\hat{h}_1(x) + r_2\hat{h}_2(x) \tag{7}$$

$$\hat{g}_2(x) = r_1\hat{h}_3(x) + r_2\hat{h}_4(x) \tag{8}$$

$$\hat{g}_3(x) = r_1\hat{h}_2(x) + r_2\hat{h}_1(x) \tag{9}$$

$$\hat{g}_4(x) = r_1\hat{h}_4(x) + r_2\hat{h}_3(x) \tag{10}$$

$$\Delta = -r_1^2 + r_2^2 \tag{11}$$

$$r_1 = i(k_1 - k_2)(1 - e^{-ik_2L}e^{-ik_2L})$$

$$r_2 = i(k_1 + k_2)(e^{-ik_2L} - e^{-ik_2L})$$

where

$$\hat{h}_1(x) = ik_2\left[e^{-ik_1x} - e^{-ik_2L}e^{-ik_1(L-x)}\right] - ik_1\left[e^{-ik_2x} - e^{-ik_1L}e^{-ik_2(L-x)}\right]$$

$$\hat{h}_2(x) = -ik_2\left[e^{-ik_2L}e^{-ik_1x} - e^{-ik_1(L-x)}\right] + ik_1\left[e^{-ik_1L}e^{-ik_2x} - e^{-ik_2(L-x)}\right]$$

$$\hat{h}_3(x) = \left[e^{-ik_1x} + e^{-ik_2L}e^{-ik_1(L-x)}\right] - \left[e^{-ik_2L} + e^{-ik_1L}e^{-ik_2(L-x)}\right]$$

$$\hat{h}_4(x) = \left[e^{-ik_2L} + e^{-ik_1x}e^{-ik_1(L-x)}\right] - \left[e^{-ik_1L}e^{-ik_2x} + e^{-ik_2(L-x)}\right]$$

Dynamic stiffness matrix

Considering the Euler-Bernoulli beam model with external excitation and nodal displacements given by $\hat{v}$ e $\hat{\phi}$ being the rotational and translational degree of freedom, respectively. Thus, the solution to equation (3) is given by,

$$\hat{v}(x,t) = A_1 e^{-ikx} + A_2 e^{-kx} + A_3 e^{ik(L-x)} + A_4 e^{k(L-x)} \tag{12}$$

Where x is the analysis point and L is the beam length. Applying the boundaries conditions to $x = 0$ and $x = L$ in the eq.18 $A_i (i = 1{:}4)$ can be obtained in function of spectral nodal displacement. The boundaries conditions can be used to write the eq.18 in matrix form,

$$\underbrace{\begin{bmatrix} 1 & 1 & e^{-ikL} & e^{-kL} \\ -ik & -k & ie^{-ikL} & e^{-kL} \\ e^{-ikL} & e^{-kL} & 1 & 1 \\ -ie^{-ikL} & -e^{-kL} & ik & k \end{bmatrix}}_{\psi} \begin{Bmatrix} A_1 \\ A_2 \\ A_3 \\ A_4 \end{Bmatrix} = \begin{Bmatrix} \hat{v}_1 \\ \hat{\phi}_1 \\ \hat{v}_2 \\ \hat{\phi}_2 \end{Bmatrix} \tag{13}$$

The spectral forces (shear force and bending moment) in the beam nodes are given by,

$$\widehat{M}(x) = +EI \frac{d^2 \hat{v}}{dx^2} \tag{14}$$

$$\hat{V}(x) = -EI \frac{d^3 \widehat{\phi}}{dx^3} \tag{15}$$

To the left side of the beam $(x = 0)$ and the right side $(x = L)$ and the nodal spectral forces can be written in the matrixial form,

$$\begin{Bmatrix} \hat{v}_1 \\ \hat{\phi}_1 \\ \hat{v}_2 \\ \hat{\phi}_2 \end{Bmatrix} = \underbrace{\begin{bmatrix} -ik^3 & k^3 & ie^{-ikL}k^3 & -e^{-kL}k^3 \\ -k^2 & k^2 & -e^{-ikL}k^2 & -e^{-kL}k^2 \\ ie^{-ikL}k^3 & -e^{-kL}k^3 & -ik^3 & k^3 \\ e^{-ikL}k^2 & -e^{-kL}k^2 & k^2 & -k^2 \end{bmatrix}}_{\Gamma} \begin{Bmatrix} A_1 \\ A_2 \\ A_3 \\ A_4 \end{Bmatrix}, \tag{16}$$

Considering the Eq. (13) and (16), the frequency dependent dynamic stiffness which relates the nodal spectral forces with the nodal spectral displacement, can be written as,

$$\{F\} = [S(\omega)]\{d(\omega)\}, \tag{17}$$

where $\{F\}$ is the vector content of the forces, $\{d(\omega)\}$ is the displacement vector and the dynamic stiffness matrix is given by,

$$[S(\omega)] = \Gamma\, \psi^{-1} \tag{18}$$

Stress-strain relation

The Bernoulli Euler beam model adopts that the deflection of the centerline $v(x,t)$ is small and only transverse. While this theory assumes the existence of a transverse shear force, it neglects any shear deformation due to it (Doyle, 2009).

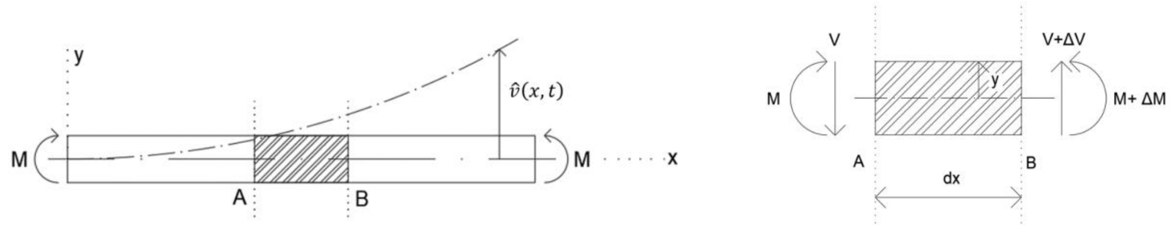

Figure 2 –Slender beam in flexure and typical loaded element.

The displacements are expanded in a Taylor series about the mid-plane displacements $\hat{u}\,(x,0)$ and $\hat{v}\,(x,0)$ as

$$\hat{u}(x,y) \approx \hat{u}(x,0) + y \frac{\partial \hat{u}}{\partial y}\Big|_{y=0} + \cdots = u(x) - y\phi(x) + \cdots \tag{19}$$

$$\hat{v}(x,y) \approx \hat{v}(x,0) + y \frac{\partial \hat{v}}{\partial y}\Big|_{y=0} + \cdots = v(x) - y\psi(x) + \cdots \tag{20}$$

The hypothesis of the Bernoulli-Euler beam is that vertical deflection is nearly constant through the thickness while the horizontal displacement follows the "plane sections remain plane" assumption. Only one term in each expansion is retained and obtain the approximate displacements as

$$\hat{u}(x,y) \approx -y\phi(x), \qquad \hat{v}(x,t) \approx v(x) \tag{21}$$

The axial strain equivalent to these deformations are

$$\epsilon_{xx} = \frac{\partial \hat{u}}{\partial x} = -y \frac{\partial \phi}{\partial x} = -y \frac{\partial^2 \hat{v}}{\partial x^2} \tag{22}$$

Entering a time-harmonic forcing in the point *x=0* of an infinite beam, tow waves are formed. The forward and backward waves, that are characterized by subscripts *i* and *r*. The two groups can be denoted as

$$v_i = \sum A e^{-i(\beta x-\omega t)} + \sum B e^{-\beta x + wt} \tag{23}$$

$$v_r = \sum C e^{i(\beta x-\omega t)} + \sum D e^{\beta x + wt} \tag{24}$$

assuming the wave propagates symmetrically outward, then at *x=0:*

$$\frac{\partial v}{\partial x} = 0, \qquad v_i = v_r$$

for the forward disturbance, the strain quantities are:

$$\epsilon_i = y \sum \beta^2 A[e^{-i\beta x} + ie^{-\beta x}]e^{i\omega t} \tag{25}$$

STRAIN MODAL ANALYSIS

Nodal displacement and strain relationship

According to (Kranjc, 2014) the strain response of a dynamical system is derived from the motion response. The motion steady-state response $\boldsymbol{X}(\omega)$ of a histerestic damped dynamical system can be written as (Ewins, 1984) and (Maia, 1997),

$$\boldsymbol{X}(\omega) = \boldsymbol{\Phi}[\omega_r^2(1+i\eta_r) - \omega^2]^{-1}\boldsymbol{\Phi}^T\boldsymbol{F}(\omega) = \boldsymbol{H}(\omega)\boldsymbol{F}(\omega) \tag{26}$$

where $\boldsymbol{\Phi}$ is the modal matrix, ω_r are the natural frequencies, η_r are the damping loss factors, $\boldsymbol{F}(\omega)$ is the vector of the excitation force, $\boldsymbol{H}(\omega)$ is the receptance matrix.

The modal solution to a Euler Bernoulli beam has the form:

$$\Phi_r = A_1 \sin(\lambda_r x) + A_2 \cos(\lambda_r x) + A_3 \sinh(\lambda_r x) + A_4 \cosh(\lambda_r x) \tag{27}$$

where the constants A_1, A_2, A_3 and A_4depend directly of the beam boundaries conditions, the subscript r relates the r^{th} mode. The value of λ_r depends on the beam properties and the natural frequency $\omega_r$of its related mode,

$$\lambda_r = \sqrt{\frac{\omega_r}{c}}, \text{ and } c = \sqrt{\frac{EI}{\rho A}} \tag{28}$$

The mode curvature k can be used to relate the displacement with strain for a bending beam. In the bending of a beam, the strain can be directly related to mode curvature as,

$$\Phi_r^\varepsilon = hk, \qquad k = \Phi'' \qquad \text{and} \qquad \Phi_r^\varepsilon = h\Phi'' \tag{35}$$

where *h* is the distance from the neutral line to the surface of the beam, ψ is the strain mode and the $''$ is the second spatial differentiation. Applying the strain mode in the Eq.(24) result to the strain steady-state response $\boldsymbol{X}^\varepsilon(\omega)$ (Bernasconi, 1989),

$$\boldsymbol{X}^\varepsilon(\omega) = \boldsymbol{\Phi}^\varepsilon[\omega_r^2(1+i\eta_r) - \omega^2]^{-1}\,\boldsymbol{\Phi}^{\boldsymbol{T}}\boldsymbol{F}(\omega) = \boldsymbol{H}^\varepsilon(\omega)\,\boldsymbol{F}(\omega) \tag{29}$$

where $\boldsymbol{H}^\varepsilon(\omega)$ is the strain Frequency Response Function (FRF) matrix and Φ^ε is the matrix of mass-normalized strain mode shapes. $\boldsymbol{H}^\varepsilon(\omega)$ can be written as (Yam et.al, 1996),

$$\boldsymbol{H}^\varepsilon(\omega) = \sum_{r=1}^{N} \frac{A_r^\varepsilon}{\omega_r^2 - \omega^2 + i\eta_r\omega_r^2} \tag{30}$$

where $\boldsymbol{A}_r^\varepsilon$ is the strain modal constants matrix, equivalent to the *r*th mode and can be written as,

$$\boldsymbol{A}_r^\varepsilon = \begin{bmatrix} \phi_{1r}^\varepsilon\phi_{1r} & \cdots & \phi_{1r}^\varepsilon\phi_{kr} & \cdots & \phi_{1r}^\varepsilon\phi_{dr} \\ \vdots & \ddots & \vdots & \ddots & \vdots \\ \phi_{jr}^\varepsilon\phi_{1r} & \cdots & \phi_{jr}^\varepsilon\phi_{kr} & \cdots & \phi_{jr}^\varepsilon\phi_{dr} \\ \vdots & \ddots & \vdots & \ddots & \vdots \\ \phi_{N_sr}^\varepsilon\phi_{1r} & \cdots & \phi_{N_sr}^\varepsilon\phi_{kr} & \cdots & \phi_{N_sr}^\varepsilon\phi_{N_dr} \end{bmatrix}_{N_d x N_s} \tag{31}$$

where ϕ_{jr}^ε and ϕ_{kr} are the components of $\boldsymbol{\Phi}_r^\varepsilon$ and $\boldsymbol{\Phi}_r$, respectively. N_d and N_s are the dimensions of $\boldsymbol{\Phi}_r$ and $\boldsymbol{\Phi}_r^\varepsilon$, respectively (Yam et.al, 1996).

Simulated Results

The parameters used in the simulation are given in Table (1), the beam is made of a steel material, free-free boundaries conditions were considered. The beam is excited by a unitary force at some point along of its length.

Table 1 – Material and geometrical properties of beam

Properties	Value [SI]
Length	1 m
Width	0,03 m
Thickness	0,005 m
Young's modulus	210×10^9 Pa
Density	7860 kg/m^3

The beam was discretized was into eight points (see fig.3), where each point has one accelerometer and one strain gauge, less the point three has just strain gauge (Santos, 2011). The experimental data was extracted from the work of Santos et al. (Santos, 2011) and the simulated results were obtained by using similar material and geometrical properties presented in their paper.

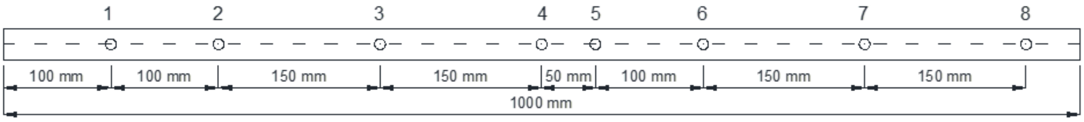

Figure 3 – Beam discretization

In the fig. 4 (a) the SFRF shows the dynamic response of a beam using the theoretical modal analysis, SEM and experimental modal analysis. The beam was excited in point 3 and measured in point 5, figure 4(a), and excited in 3 and measured in point 8, figure 4(b). By comparing the numerical methods, SEM and theoretical modal analysis presented similar resonance picks and close mode shapes with exception of the amplitudes at the two firsts resonance frequencies. By comparing the numerical methods with the experimental SFRF obtained by the experimental modal analysis, there is a small discrepancy at the first and second resonance frequencies, it is related with the randomness in boundary condition that would not be considered in the numerical model. From frequency, 100Hz is seeing a lot of noise in the experimental data. However, the methods showed a small difference, the SEM had a good response in obtained the SFRF. That advantage in using the proposed technique to numerically estimated de SFRS is because, SEM calculates directly the SFRF and, once it is formulated based on the analytical wave solution the dynamic response has an accurate solution.

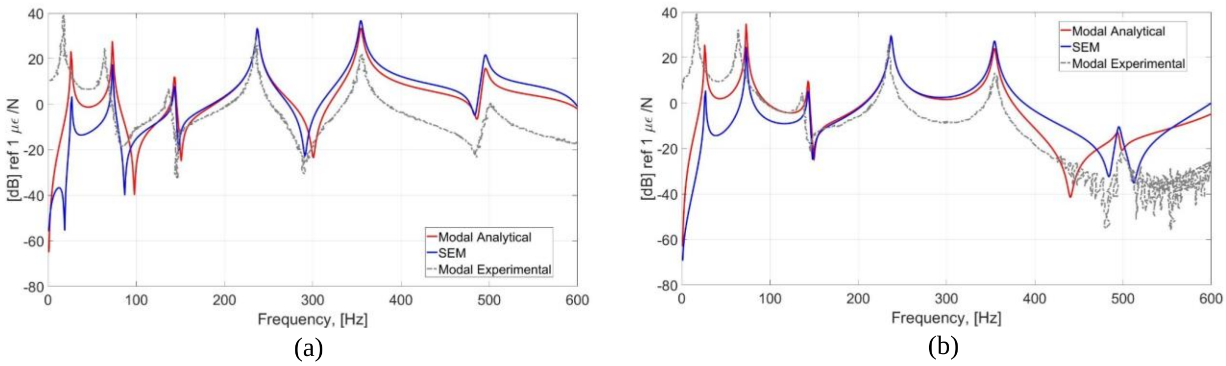

Figure 4 (a) – Beam SFRF using three different methods, modal analytical, SEM and Modal experimental. In (a), the excitation was inserted in the point 3 and measurement done the point 5 and in (b) the excitation was maintained in point 3 and the measurement was done in the point 8.

The experimental modal data to calculate the SFRF using the modal analysis were taken from (Santos, 2011). The strain modal shape was obtained by measured the strain deformation through 8 strain gauges set along the beam. To obtain the modal shape, the dimension, material properties and boundaries conditions of the experimental test and the numerical simulations are the same.

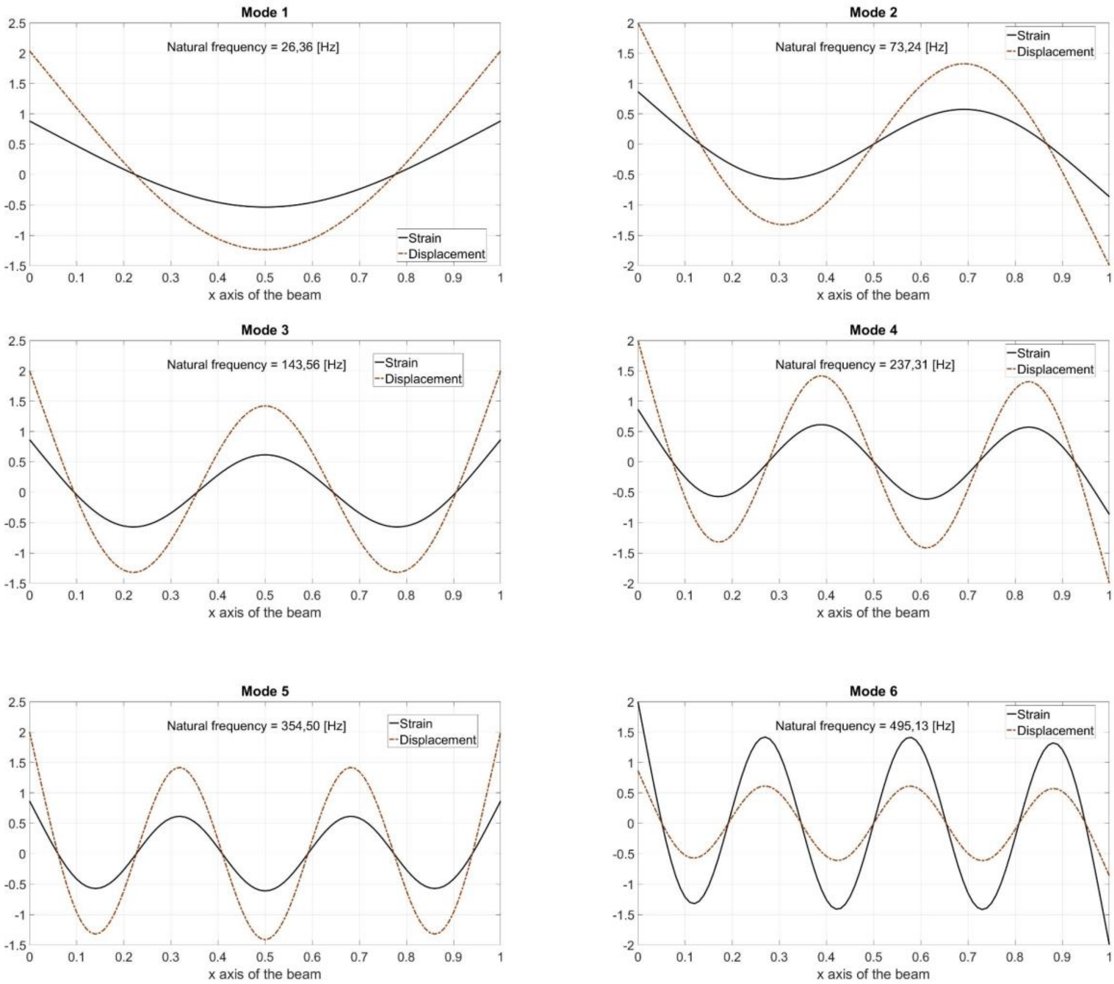

Figure 5 –1º to 6º displacement modes shapes (--) and strain modes shapes (–), obtained through the analytical modal analyses.

Figure 5 shows the 1st to 6th displacement and strain modal shapes. For each mode shape the related to correspondent ressonance frequency is showed in Table 2 and Table 3.

Table 2 – Resonance frequency by mode for SEM, modal analytical and modal experimental methods.

Mode	Frequency [Hz]		
	SEM	Modal Analytical	Modal Experimental
1	26,54	26.36	17,10
2	73,24	73,24	64,37
3	143,50	143,56	136,32
4	237,40	237,31	234,4
5	354,40	354,50	354,3
6	495,55	495,13	495,8

Table 3 – Resonance frequency by mode comparing SEM and modal analytical methods.

Mode	Frequency [Hz]		Error [%]
	SEM	Modal Analytical	
1	26,54	26.36	0,68
2	73,24	73,24	0
3	143,50	143,56	0,04
4	237,40	237,31	0,03
5	354,40	354,50	-0,02
6	495,15	495,13	0,01

Table 4 – Resonance frequency by mode comparing SEM and modal experimental methods.

Mode	Frequency [Hz]		Error [%]
	SEM	Modal Experimental	
1	26,54	17,10	55,20
2	73,24	64,37	13,77
3	143,50	136,32	5,26
4	237,40	234,4	1,27
5	354,40	354,3	0,02
6	495,55	495,58	-0,01

In Table 2 the six resonance frequency correspondent to each mode obtained by SEM, theoretical modal analysis, and experimental modal analysis are compared. Table 3 and 4 comparing SEM with theoretical modal analysis, and SEM compared to experimental modal analysis, respectively. The maximum relative error between the two numerical methods was 0.68%. By comparing the SEM with the experimental data, Table 4, for the first and second frequencies, the error was 55% and 13% respectively, for the 3rd to 6th the maximum relative error was 5%. The high error in the first resonance frequency is due the boundary condition.

CONCLUSIONS

In this research, we considered the SFRF using SEM, as an alternative method to analyses the strain dynamic behavior. The SFRF usually is obtained by modal analytical, in numerical cases and modal experimental at experimental cases. In modal experimental is used the strain gauges to measure the structure response. These works proposed the use of SEM in the SFRF formulation.

Approximated results between the SEM and the modal analytical. In all frequencies the response of both methods is similar showing that the theoretical model for both methods are equivalents. In the SEM and modal experimental comparations, the results had a high error in low frequency, that can be caused by boundaries conditions of the experiment or simply the imprecision of both methods in low frequency. The precision of the SEM increases with the frequency.

REFERENCES

Doyle, J.F., 1997. “Wave propagation in structures: spectral analysis using fast discrete Fourier transforms”. Mechanical engineering. Springer-Verlag New York, Inc., New York, 2nd edition.

Machado, M.R. and DosSantos, J.M.C., 2012**.** “Wave propagation in a cracked beam spectral element including parameter uncertainty”. In Proceedings of the 1st International Symposium on Uncertainty Quantification and Stochastic Modeling.

Lee, U., 2009. “Spectral element method in structural dynamics” John Wiley & Sons, Inha University, Republic of Korea.

Santos, F.L.M, 2011. “strain-based experimental modal analysis: use of mode curvature and strain-to-displacement relations”, Siemens Industry Software, Leuven, Belgium.

D. Ewins, 1984. “Modal testing: Theory and practice, Mechanical engineering research studies: Engineering dynamics series”, Research Studies Press.

N. Maia, J. Silva, 1997 “Theoretical and Experimental Modal Analysis, Mechanical Engineering Research Studies: Engineering Dynamics Series”, John Wiley& Sons, Limited.

L. Yam, T. Leung, 1996. D. Li, K. Xue, “Theoretical and experimental study of modal strain analysis”, Journal of Sound and Vibration 191 (2) 251 – 260.

Kranjc, T., Slaviˇc, J. and Bolteˇzar, M., “The mass normalization of the displacement and strain mode shapes in a strain experimental modal analysis using the mass-change strategy”, Journal of Sound and Vibration, Volume 332, Issue 26, 23 December 2013, Pages 6968-6981, ISSN 0022-460X, http://dx.doi.org/10.1016/j.jsv.2013.08.015.

O. Bernasconi, D. J. Ewins, 1989. “Application of strain modal testing to real structures”, In: Proceedings of the 7th International Modal Analysis Conference (IMAC-VII), pp. 1453–1464.